

PERFORMANCE OF THE DIGITAL LLRF SYSTEMS AT KEK cERL

F. Qiu[#], D. Arakawa, Y. Honda, H. Katagiri, T. Matsumoto, S. Michizono, T. Miura, T. Obina, H. Sakai, KEK, Tsukuba, Ibaraki 305-0801, Japan
 S. B. Wibowo, SOKENDAI, The Graduate University for Advanced Studies, Hayama, Kanagawa 240-0193, Japan

Abstract

A compact energy recovery linac (cERL), which is a test machine for the next generation synchrotron light source 3-GeV ERL, was constructed at KEK. In the cERL, a normal conducting (NC) buncher cavity and three superconducting (SC) two-cell cavities were installed for the injector, and two nine-cell SC cavities were installed for the main linac (ML). The radio-frequency (RF) fluctuations for each cavity are required to be maintained at less than 0.1% rms in amplitude and 0.1° in phase. These requirements are fulfilled by applying digital low-level radio-frequency (LLRF) systems. During the beam-commissioning, the LLRF systems were evaluated and validated. A measured beam momentum jitter of 0.006% shows that the target of the LLRF systems is achieved. To further improve the system performance, an adaptive feedforward (FF) control-based approach was proposed and demonstrated in the beam-commissioning. The current status of LLRF system and the adaptive FF approach for LLRF control in the cERL are presented in this paper.

INTRODUCTION

At KEK, a compact energy recovery linac (cERL), as a test facility for future 3-GeV ERL project, was constructed, and the first beam-commissioning was carried out at June, 2013 [1, 2]. The cERL is a 1.3 GHz superconducting radio-frequency (SCRF) machine that is operated in continuous-wave (CW) mode. As shown in Fig. 1, the cERL consists of an injector part and a main linac (ML) part. A normal conducting (NC) cavity (buncher) and three two-cell superconducting (SC) cavities (Inj. 1, Inj. 2, and Inj. 3), were installed in the injector, and two main nine-cell SC cavities (ML1 and ML2) were installed in the main linac (ML). For low-emittance beam, the requirements of the RF field stabilities are 0.1% rms in amplitude and 0.1° in phase in the cERL. This requirements are fulfilled by applying digital low-level radio-frequency (LLRF) systems.

The LLRF system in the cERL is disturbed by various disturbances include the 50-Hz microphonics, the 300-Hz high-voltage power supply (HVPS) ripples and the burst mode beam-loading [3-4]. The current LLRF system is not sufficient to reject all of these disturbances. In view of this situation, we have proposed a disturbance observer (DOB)-based approach for suppress the main disturbances in the cERL [3]. Based on this approach, the disturbances can be reconstructed by the cavity pickup signal and then removed from the feedforward (FF) table in real-time. Therefore, in terms of function, this approach

is just like an adaptive FF control.

In this paper, we first introduce the LLRF system in the cERL, and then present the measured LLRF stability and beam momentum jitter during the cERL beam-commissioning. In the next stage, we describe the basic idea of the proposed adaptive FF approach for disturbances rejection. Finally, we present the preliminary result of this adaptive FF approach for microphonics rejection in the cERL commissioning.

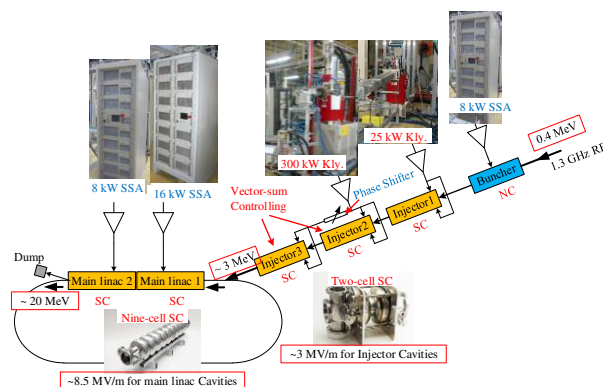


Figure 1: Layout of the cavities in the cERL. The marked values of beam energy and accelerating field indicate the current state in the cERL beam-commissioning.

HLRF SYSTEM

RF power sources including 25 kW klystron, 300 kW klystron, 8 kW solid state amplifier (SSA) and 16 kW SSA were employed in the cERL. Figure 1 shows the layout of the cavities and corresponding power sources in the cERL. Table 1 gives the loaded Q value, required RF power, and RF sources for each cavity. It should be mentioned that, in the Inj. 2 and Inj. 3, a vector-sum control method is applied. All of these RF sources are stable and reliable in the beam commissioning.

Table 1: Cavity Parameters of the cERL

Cav.	Q_L	$f_{1/2}$ [Hz]	RF power [kW]	RF source
Bun.	1.1×10^4	57000	3	8 kW SSA
Inj. 1	1.2×10^6	540	0.53	25 kW Kly.
Inj. 2	5.8×10^5	1120	2.4	300 kW Kly.
Inj. 3	4.8×10^5	1350		
ML1	1.3×10^7	50	1.6	16 kW SSA
ML2	1.0×10^7	62	2	8 kW SSA

[#]qiufeng@post.kek.jp

LLRF SYSTEM

A simplified schematic of the cEERL LLRF system is shown in Fig. 1. The 1.3-GHz cavity pick up signal is down-converted to a 10-MHz intermediate frequency (IF) signal at first. The 10-MHz IF signal is sampled at 80-MHz by a 16-bit analog to digital converter (ADC) and then fed into a field-programmable gate array (FPGA) board. The baseband in-phase and quadrature (I/Q) components are detected from the IF signal with a non-IQ-based IQ detection method. After being filtered by infinite impulse response (IIR) filters, the detected I/Q signals are compared with their set values, and the I/Q error signals are calculated. The I/Q error signals are controlled by proportional and integrational (PI) feedback (FB) controllers and then added together with their corresponding FF tables. Finally, the combined I/Q signals are fed into an I/Q modulator via 16-bit digital to analog convertors (DACs) to regenerate the 1.3-GHz RF signal. This regulated RF signal will be used to drive the high-power RF source (e.g. klystron and SSA), which drives the cavities. It should be mentioned that, to evaluate the stability of the cavity pick-up signal, we have installed a pick-up monitor inside FPGA (see Fig. 2). An adjustable-bandwidth digital filter, aims to remove the ADC noises, is placed in front of the monitor.

A μ TCA system is employed as the digital control platform. Experimental physics and industrial control system (EPICS) is selected to be the data communication system. The detailed information about that digital platform can be found in [4].

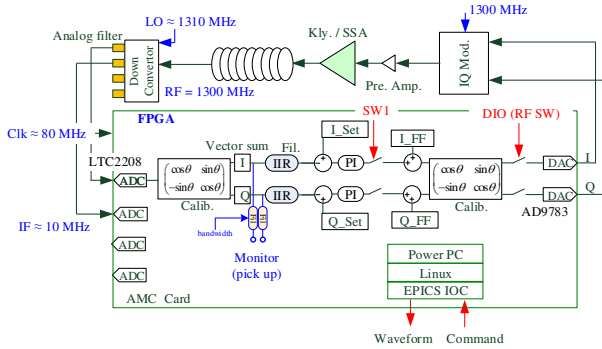


Figure 2: Schematic of the LLRF system in the cEERL.

STABILITY

The typical LLRF system performance in the cEERL beam-commissioning are listed in Table 2. Generally speaking, all of our LLRF systems satisfy the requirements of the cEERL beam-commissioning. Disturbances in the LLRF system are suppressed well by applying high FB gains. However, some high intensity disturbances still exist in the LLRF systems. Figure 3 shows the RF performance of Inj. 2&3 and ML2. It is very clearly to see that, there is a 300-Hz fluctuation in the vector-sum RF field of Inj. 2&3 cavities, especially in the phase. Investigations reveal that this 300-Hz ripples come from the high voltage power supply [3]. On the other hand, an approximately 50-Hz component can be

observed in the phase of the ML2, this component is mainly caused by the microphonics [5].

The beam energy stability is measured by the screen monitor which is installed downstream of the bending magnet with a 2.2 m dispersion and 62.6 $\mu\text{m}/\text{pixel}$ resolution. The beam momentum jitter is calculated based on the peak point of the beam projection in the screen monitor. The calibrated beam momentum jitter is about 0.006% rms as shown in Fig. 4. This value is in consistence with the measured RF stability in the LLRF system (see Table 2).

Table 2: Status of RF Systems in the Commissioning

Cavity	φ_b	V_c	RF stability (rms)	
			$\delta A/A$	$\delta\theta$
Buncher	-90°		0.07%	0.04°
Inj. 1	0°	0.7 MV	0.006%	0.009°
Inj. 2	0°	0.65 MV	0.007%	0.025°
Inj. 3	0°	0.65 MV		
ML1	0°	8.56 MV	0.003%	0.010°
ML2	0°	8.56 MV	0.003%	0.007°

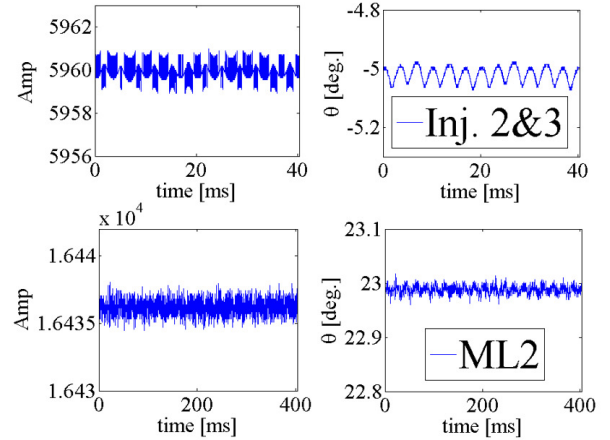


Figure 3: RF stability of the Inj. 2&3 (top) and ML2 (bottom). The 300-Hz fluctuation in the Inj. 2&3 is caused by the high voltage power supply ripples.

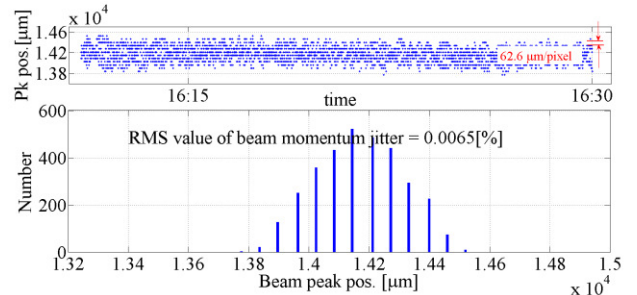


Figure 4: Beam momentum jitter measurement. The measured beam momentum jitter was 0.0065% rms, which is in agreement well with RF stability.

ADAPTIVE FF CONTROL

As depicted in Fig. 3, disturbances still exist in the current LLRF system even with high FB gains. These disturbance signals can be rejected clearly by applying an adaptive FF approach. The key idea of this adaptive FF approach is as bellow.

1. Identify the nominal system model and calculate its inverse model.
2. Estimate and rebuild the disturbance signals based on the inverse model in the step 1 from cavity pickup signal.
3. Remove the estimated disturbance in step 2 from the FF table inside FPGA.

The first step is performed off-line, whereas the next two steps are carried out in real-time. Therefore, the disturbances are removed in the cavity pickup signal. This process can be illustrated in Fig. 5. Here, $G_p(s)$ and $G_n(s)$ represent the actual plant (e.g., cavities and RF devices) and nominal model, respectively. Signals d and d_e represent the real disturbance and the disturbance estimate, respectively. Signal FF represents the FF table output. As shown in Fig. 5, the disturbance estimate d_e can be expressed by [3]

$$d_e = (\varepsilon + d)G_p(s)G_n^{-1}(s) - \varepsilon. \quad (1)$$

If the system nominal model $G_n(s)$ is a perfect representation of real system $G_p(s)$, then according to (1), the $G_p(s)$ is perfectly cancelled by $G_n^{-1}(s)$, therefore, the disturbance estimate d_e is exactly equal with real disturbance d , that means, the disturbance d is perfectly rebuilt by disturbance estimate d_e . In practice, the system model cannot be identified perfectly, this is to say, there are some deviations between real disturbance d and d_e . Fortunately, a related analytical study reveals that the robustness of this approach is rather strong, that means the adaptive FF controller still works well even in the presence of the model mismatch.

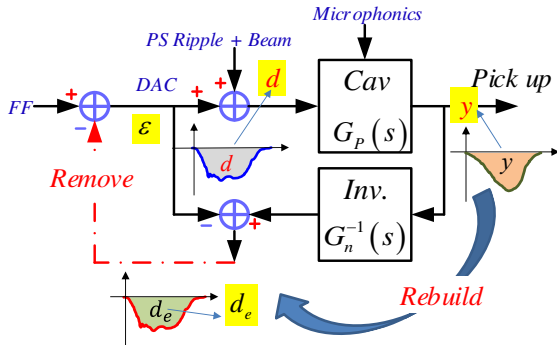


Figure 5: Basic idea of the adaptive FF approach, the key step is to reconstruct the disturbances based on the inverse system model.

We have developed and installed this adaptive FF controller in the cERL μ TCA-bases LLRF systems. During the beam-commissioning, we have demonstrated this approach for disturbance rejection. As presented above, in the cERL, the main disturbances in the LLRF

systems include the 300 Hz power supply ripples, the high intensity beam-loading, and the microphonics. Concerning the validation of the adaptive FF controller regards to power supply ripples rejection and beam-loading compensation, the preliminary results were already presented in [3]. For microphonics rejection for the ML2 cavity, the performance of the adaptive FF control is shown in Fig. 6. If we only use traditional PI control but without the adaptive FF control (indicated by the blue color in Fig. 6), the microphonics effect of ML2 cavity can be observed clearly in the phase of the RF field. It is clear to see that there is a 50 Hz dominant component in both waveform and spectrum in the RF phase of the ML2 cavity. After switching on the adaptive FF control, the microphonics include the 50-Hz dominant component are disappeared (indicated by the red color in the Fig. 6).

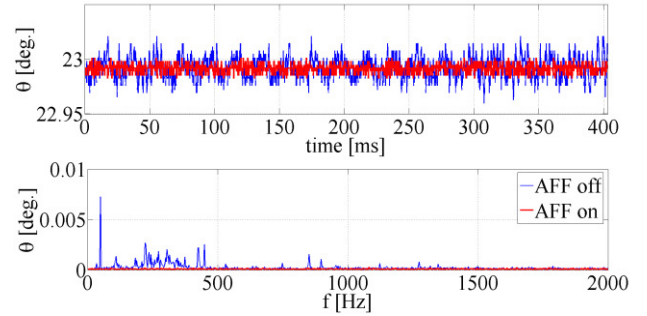


Figure 6: Measured RF phase of the ML2 cavity pickup signal in the case of with and without adaptive FF control. Both waveform (top) and spectrum (bottom) are presented.

SUMMARY

Digital LLRF systems for the injector and main linac were constructed in the cERL at KEK. During the beam-commissioning, the LLRF systems perform well and the required RF stability of the cERL (0.1% rms in amplitude and 0.1° in phase) is satisfied. Furthermore, a beam momentum jitter of approximately 0.006% was achieved. Additionally, for R&D, we have proposed an adaptive FF-based approach aims to reject the disturbances in the RF system. Results in the cERL commissioning show that this approach is very effective for the disturbance rejection.

REFERENCES

- [1] N. Nakamura et al., "Present status of the compact ERL at KEK," Proc. IPAC'14, Dresden, Germany (2014).
- [2] S. Sakanaka et al., "Construction and commissioning of compact-ERL Injector at KEK," Proc. ERL2013, Novosibirsk, Russia (2013).
- [3] F. Qiu et al., "A disturbance-observer-based controller for LLRF systems", Proc. IPAC'15, Richmond, USA (2015).
- [4] T. Miura, "Low-level RF system for cERL", Proc. IPAC'10, Kyoto, Japan (2010).

- [5] M. Satoh et al., “Mechanical vibration search of compact ERL main linac superconducting cavities in crymodule”, Proc. IPAC’14, Dresden, Germany (2014).